On Procrustes Analysis in Hyperbolic Space

Puoya Tabaghi and Ivan Dokmanić, *Member, IEEE*

***Abstract*—Congruent Procrustes analysis aims to find the best matching between two point sets through rotation, reflection and translation. We formulate the Procrustes problem for hyperbolic spaces, review the canonical definition of the center mass for a point set, and give a closed-form solution for the optimal isometry between noise-free point sets. Our algorithm is analogous to the Euclidean Procrustes analysis, with centering and rotation replaced by their hyperbolic counterparts. When the data is corrupted with noise, our algorithm computes a sub-optimal alignment. We thus propose a gradient-based fine-tuning method to improve the matching accuracy.**

***Index Terms*—Hyperbolic geometry, procrustes analysis.**

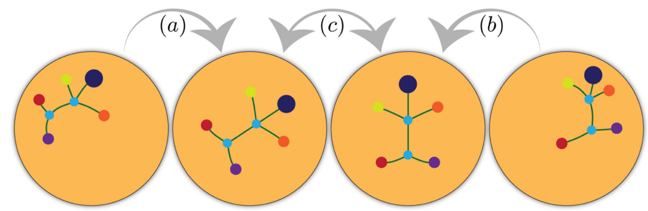

Fig. 1. Tree alignment in the Poincaré disk [24]. Hyperbolic Procrustes analysis aims to align the far left and far right trees. In steps (a) and (b) we center vertices in both trees, while in (c) we estimate the unknown rotation.

I. Introduction

In GREEK mythology, Procrustes was a robber who lived in Attica and deformed his victims to match the size of his bed. In 1962, Hurley and Catell used the story of Procrustes to describe a point set matching problem in Euclidean spaces [1], stated below.

Problem 1: Let $\{z_n\}_{n=1}^N$ and $\{z'_n\}_{n=1}^N$ be two point sets in $\mathbb{R}^d$. The Procrustes problem asks to find a map $\widehat{T}$ that minimizes the sum of the mismatch norms, i.e.,

$$\widehat{T} = \arg\min_{T \in \mathcal{T}} \sum_{n=1}^{N} \|z_n - T(z'_n)\|_2^2$$

where $\mathcal{T}$ is the set of rotation, reflection, translation, and uniform scaling maps and their compositions [2].

In computer vision, Procrustes analysis is of relevance in point cloud registration problems. The task of rigid registration is to find an isometry between two (or more) sets of points sampled from a 2 or 3 dimensional object. Point registration has applications in object recognition [3], medical imaging [4] and localization of mobile robotics [5]. Procrustes problems also naturally arise in distance geometry problems [6], [7] where one wants to find the location of a point set that best represents a given set of incomplete point distances, i.e.,

$$z_1, \ldots, z_N \in \mathbb{R}^d : \|z_n - z_m\| = d_{mn},\ \forall (m,n) \in \mathcal{M}$$

where $\mathcal{M} \subset \{1, \ldots, N\}^2$ and $\{d_{m,n} : (m,n) \in \mathcal{M}\}$ is the set of measured distances [8]. If a distance geometry problem has a solution, it is an orbit of the form

$$O_{\mathcal{Z}} = \{\{T(z_n)\}_{n=1}^N \text{ s.t. } T : \mathbb{R}^d \to \mathbb{R}^d \text{ is an isometry}\},$$

where $\mathcal{Z} = \{z_n\}_{n=1}^N$ is a particular solution. In order to uniquely identify the correct solution in the orbit $O_{\mathcal{Z}}$, we may be given the exact position of a subset of points, called *anchors*. We use Procrustes analysis to pick the correct solution by finding the best match between the anchors with their corresponding points in the orbit.

Procrustes analysis can be performed in any metric space. In particular, hyperbolic Procrustes analysis is of great relevance due to the recent surge of interest in hyperbolic embeddings and machine learning [9]–[16]. Furthermore, hyperbolic embeddings are closely connected to the study of hierarchical or tree-like data structures and hyperbolic Procrustes problem solutions may be used to align hierarchical data, e.g., ontologies and phylogenies [17]–[19]. The goal of ontological studies is to find a map between a fixed number of entities in two heterogeneous tree-like structures that are best semantically aligned to each other [17] (see Fig. 1 for an illustration). In natural language processing, this alignment objective can be used for cross-lingual information retrieval [20]. Lastly, recent efforts to embed and analyze phylogenetic trees in hyperbolic spaces [10], [21] motivate the need to generalize phylogenetic tree matching methods [22], [23] to hyperbolic spaces.

In unsupervised matching problems, the first step in Procrustes-type analyses is to find the correspondence between two point clouds by using the iterative closest point algorithm [25]. The recent optimal-transport based methods [26], [27] tackle the unsupervised hierarchy matching problem in hyperbolic spaces. These methods aim to jointly learn the "soft" correspondence and the alignment map characterized by a hyperbolic neural network. In this paper, we propose an *algebraic* solution for the hyperbolic alignment map.

Specifically, we find an isometry that best aligns two noise-free hyperbolic point sets, i.e., a supervised matching problem. We can decompose a hyperbolic isometry into elementary maps of translation and rotation (and reflection). Then, we aim to jointly estimating each map. We proceed by reviewing the definition of the *centroid* for a point set in hyperbolic spaces.

Manuscript received February 22, 2021; revised April 19, 2021; accepted May 2, 2021. Date of publication May 18, 2021; date of current version June 14, 2021. The associate editor coordinating the review of this manuscript and approving it for publication was Prof. Dezhong Peng. *(Corresponding author: Puoya Tabaghi.)*

Puoya Tabaghi is with the Coordinated Science Lab, University of Illinois at Urbana-Champaign IL USA, (e-mail: tabaghi2@illinois.edu).

Ivan Dokmanić is with the Department of Mathematics and Computer Science, University of Basel,, Switzerland (e-mail: ivan.dokmanic@unibas.ch).

Digital Object Identifier 10.1109/LSP.2021.3081379

This work is licensed under a Creative Commons Attribution 4.0 License. For more information, see https://creativecommons.org/licenses/by/4.0/

This enables us to decouple the joint estimation problem into two steps: (1) "center" each point set, and (2) estimate the unknown rotation factor.

While hyperbolic centering has been studied in the literature [28], our Procrustes analysis framework is different from prior work in so far that it is similar to its Euclidean counterpart, and provides the optimal estimate for the unknown rotation factor. Moreover, we prove that our proposed method returns the optimal isometry if the point sets perfectly match. We conclude the paper by giving numerical performance bounds for the task of matching noisy point sets.

Summary: Let $\{x_n\}_{n\in[N]}$, and $\{x'_n\}_{n\in[N]}$ be two sets of points in a hyperbolic space, related through an isometric map, i.e., $x'_n = T(x_n), \forall n \in [N]$. Then,

$$T = T_{m_{x'}} \circ T_U \circ T_{-m_x}$$

where $m_x, m_y \in \mathbb{R}^d$ are each sets' centroids, T_b is the translation map by vector $b \in \mathbb{R}^d$, and T_U is a rotation map by a unitary matrix $U \in \mathbb{O}(d)$; see Section III. For noisy points, this isometry is suboptimal (in ℓ_2 sense) and can be fine-tuned via a gradient-based algorithm.

Notation: For $N \in \mathbb{N}$, we let $[N] = \{1, \ldots, N\}$. Depending on the context, x_1 can either be the first element of $x \in \mathbb{R}^d$, or an indexed vector. We denote the set of orthogonal matrices as $\mathbb{O}(d) = \{R \in \mathbb{R}^{d\times d} : R^\top R = I\}$. For a function f and its inputs $x_1, \ldots, x_N$, we write $\overline{f(x_n)} = \frac{1}{N}\sum_{n\in[N]} f(x_n)$. For a vector $b \in \mathbb{R}^d$, we denote its ℓ_2 norm as $\|b\|_2$.

II. 'Loid Model of Hyperbolic Space

Let $x, x' \in \mathbb{R}^{d+1}$ with $d \geq 1$. The Lorentzian inner product between x and x' is defined as

$$[x, x'] = x^\top H x' : H = \begin{pmatrix} -1 & 0^\top \\ 0 & I_d \end{pmatrix}, \quad (1)$$

where $I_d \in \mathbb{R}^{d\times d}$ is the identity matrix, and $0 \in \mathbb{R}^d$ is a zero vector. This is an indefinite inner product on $\mathbb{R}^{d+1}$. The vector space $\mathbb{R}^{d+1}$ equipped with the Lorentzian inner product is called a Lorentzian $(d+1)$-space. In a Lorentzian space, we can define notions similar to adjoint and unitary matrices in Euclidean spaces. The H-adjoint of the matrix R, denoted by $R^{[*]}$, is defined via

$$[Rx, x'] = [x, R^{[*]}x'], \quad \forall x, x' \in \mathbb{R}^{d+1},$$

or simply as $R^{[*]} = H^{-1}R^\top H$. An invertible matrix R is called H-unitary if $R^{[*]} = R^{-1}$ [29].

The 'Loid model of d-dimensional hyperbolic space is a Riemannian manifold $\mathcal{L}^d = (\mathbb{L}^d, (g_x)_x)$, where

$$\mathbb{L}^d = \{x \in \mathbb{R}^{d+1} : [x, x] = -1, x_1 > 0\}$$

and the Riemannian metric $g_x : T_x\mathbb{L}^d \times T_x\mathbb{L}^d \to \mathbb{R}$ is defined as $g_x(u, v) = [u, v]$. The distance function in the 'Loid model is characterized by Lorentzian inner products as

$$d(x, x') = \operatorname{acosh}(-[x, x']), \forall x, x' \in \mathbb{L}^d.$$

A. Isometries

A map $T : \mathbb{L}^d \to \mathbb{L}^d$ is an isometry if it is bijective and preserves distances, i.e. if

$$d(x, x') = d\left(T(x), T(x')\right), \quad \forall x, x' \in \mathbb{L}^d.$$

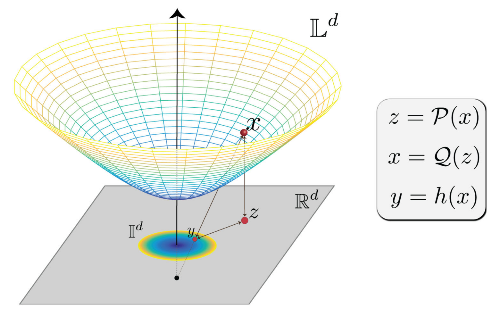

Fig. 2. Geometric illustration of $\mathcal{P}$, $\mathcal{Q}$, and stereographic projection h.

We can represent any hyperbolic isometry as a composition of two *elementary* maps that are parameterized by a d-dimensional vector and a $d \times d$ unitary matrix, as described in Fact 1.

Fact 1: [30] The function $T : \mathbb{L}^d \to \mathbb{L}^d$ is an isometry if and only if it can be written as $T(x) = R_U R_b x$, where

$$R_U = \begin{bmatrix} 1 & 0^\top \\ 0 & U \end{bmatrix}, \; R_b = \begin{bmatrix} \sqrt{1 + \|b\|_2^2} & b^\top \\ b & (I + bb^\top)^{\frac{1}{2}} \end{bmatrix}$$

for a unitary matrix $U \in \mathbb{O}(d)$ and a vector $b \in \mathbb{R}^d$.

Fact 1 can be directly verified by finding the conditions for a real matrix R such that $R^\top H R = H$, or simply $R = H^{-\frac{1}{2}} C H^{\frac{1}{2}} \in \mathbb{R}^{(d+1)\times(d+1)}$ where $C^\top C = I_{d+1}$ and $C \in \mathbb{C}^{(d+1)\times(d+1)}$. We use this parametric decomposition of rigid transformations to solve the Procrustes problem in $\mathbb{L}^d$.

The hyperbolic translation map $T_b : \mathbb{L}^d \to \mathbb{L}^d$ and hyperbolic rotation map $T_U : \mathbb{L}^d \to \mathbb{L}^d$ are defined as

$$T_b(x) = R_b x, \quad T_U(x) = R_U x, \quad (2)$$

where $b \in \mathbb{R}^d$ and $U \in \mathbb{O}(d)$. It can be easily shown that $T_b^{-1} = T_{-b}$ and $T_U^{-1} = T_{U^\top}$.

III. Procrustes Analysis

Euclidean (orthogonal) Procrustes analysis proceeds through two steps:

- Centering: moving the center of mass of both points set to the origin of Cartesian coordinates, and
- Finding the optimal rotation/reflection.

We proceed to review (and visualize) the definition of the center of mass of a point set in hyperbolic space [28, Chapter 13].

We start by projecting each point $x \in \mathbb{L}^d$ onto the following d-dimensional subspace

$$H_d = \{x \in \mathbb{R}^{d+1} : x_1 = 0\}.$$

Then, we can simply neglect the first element of the projected point (which is always zero), and define a one-to-one map $\mathcal{P}$ between $\mathbb{L}^d$ and $\mathbb{R}^d$; see Fig. 2. In Definition 1, we formalize this projection and its inverse.

Definition 1: The projection operator $\mathcal{P} : \mathbb{L}^d \to \mathbb{R}^d$ and its inverse $\mathcal{Q}$ are defined as

$$\mathcal{P}\left(\begin{bmatrix} \sqrt{1 + \|z\|^2} \\ z \end{bmatrix}\right) = z, \; \mathcal{Q}(z) = \begin{bmatrix} \sqrt{1 + \|z\|^2} \\ z \end{bmatrix}.$$

For brevity, we define $\mathcal{P}(X) \underset{=}{\text{def}} [\mathcal{P}(x_1), \ldots, \mathcal{P}(x_N)]$ where $X = [x_1, \ldots, x_N] \in (\mathbb{L}^d)^N$. Similarly, we consider this extension for $\mathcal{Q}$ as well.

In Section III-A, we review the hyperbolic centering process [28]. In other words, we find a map T_b to move the center of mass of projected point sets to $0 \in \mathbb{R}^d$, i.e., $\overline{\mathcal{P}(T_b(x_n))} = 0$. Then, we show how this centering method helps simplify the hyperbolic Procrustes problem to a sub-problem similar to the famous (Euclidean) orthogonal Procrustes problem.

A. Hyperbolic Centering

In Euclidean Procrustes analysis, we have two point sets $z_1, \ldots, z_N$ and $z'_1, \ldots z'_N$ that are related via a composition of rotation, reflection, and translation maps, i.e.,

$$z_n = U z'_n + b$$

where $U \in \mathbb{O}(d)$ and $b \in \mathbb{R}^d$. We extract translation invariant features by moving their center to $0 \in \mathbb{R}^d$, i.e., $z_n - \overline{z_n} = U(z'_n - \overline{z'_n})$. The main purpose of centering is to map each point set to new locations, $z_n - \overline{z_n}$ and $z'_n - \overline{z'_n}$ that are invariant with respect to the unknown translation b. Subsequently, we can estimate the unknown unitary matrix $\hat{U}$, and then the translation according to $\widehat{b} = \overline{z_n} - \widehat{U}\overline{z'_n}$.

In hyperbolic Procrustes analysis, we have

$$x_n = R_b R_U x'_n, \forall n \in [N] \tag{3}$$

where $U \in \mathbb{O}(d)$ and $b \in \mathbb{R}^d$. In a similar way, we pre-process a point set to extract (hyperbolic) translation invariant locations, i.e., centered point sets. Lemma 1 gives a simple method to center a projected point set.

Lemma 1: [28] Let $x_1, x_2, \ldots, x_N \in \mathbb{L}^d$. Then, we have $\overline{\mathcal{P}(R_{-m_x} x_n)} = 0$, where $m_x \overset{\text{def}}{=} \frac{1}{\sqrt{-[\overline{x_n}, \overline{x_n}]}} \overline{\mathcal{P}(x_n)}$.

In Proposition 1, we show that T_{-m_x} is the canonical translation map for centering the point set $X \in (\mathbb{L}^d)^N$.

Proposition 1: Let $x_1, \ldots, x_N$ and $x'_1, \ldots x'_N$ in $\mathbb{L}^d$ such that

$$x_n = R_b R_U x'_n, \ \forall n \in [N].$$

for $b \in \mathbb{R}^d$ and $U \in \mathbb{O}(d)$. Then, $R_{-m_x} x_n = R_V R_{-m_{x'}} x'_n$ where R_V is a hyperbolic rotation matrix.

Proof: From Lemma 1, we have

$$\overline{R_{-m_x} x_n} = \begin{bmatrix} a \\ 0 \end{bmatrix}, \overline{R_{-m_{x'}} x'_n} = \begin{bmatrix} a' \\ 0 \end{bmatrix}$$

for $a, a' \in \mathbb{R}$. We can rewrite (3) in the following form

$$R_{-m_x} x_n = R' R_{-m_{x'}} x'_n, \forall n \in [N].$$

where $R' = R_{-m_x} R_b R_U R_{m_{x'}}$. Since R' is an H-unitary matrix, we can decompose it as $R' = R_c R_V$ for some $c \in \mathbb{R}^d$ and $V \in \mathbb{O}(d)$. Therefore, we have

$$\begin{bmatrix} a \\ 0 \end{bmatrix} = R_c R_V \begin{bmatrix} a' \\ 0 \end{bmatrix} \Rightarrow c = 0.$$

∎

The map T_{-m_x} not only centers a set of points, but also rotates them. This phenomenon is rooted in the noncommutative property of hyperbolic translation or *gyration*. More clearly, for any two vectors $b_1, b_2 \in \mathbb{R}^d$, we have

$$R_{b_1} R_{b_2} = R_V R_{b_2} R_{b_1}$$

for a specific unitary matrix $V \in \mathbb{O}(d)$ that accounts for the *gyration* factor; see the example in Fig. 3 and the follow-up discussion in Section III-C. This does not interfere with our analysis since any such rotation is absorbed in U and we can estimate the *effective* unitary transformation.

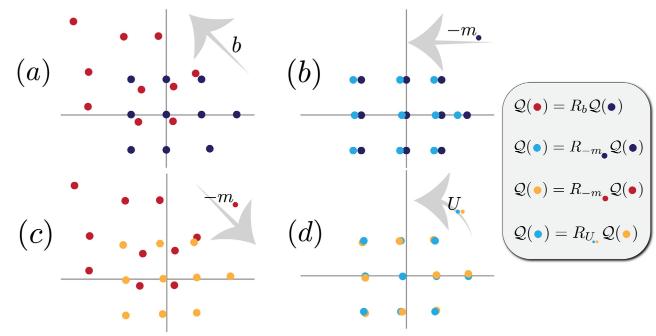

Fig. 3. (a): Red and blue are projected points related by a translation, i.e., $X = R_b X'$. (b, c): Centering each point set. (d): Centered points are related via a rotation, i.e., $R_{m_x} R_b R_{-m_{x'}} \neq I_d$.

Now, let us consider the following noisy case,

$$x_n = R_b R_U R_{\epsilon_n} x'_n, \ \forall n \in [N]$$

where $\epsilon_n \in \mathbb{R}^d$ is a translation noise for the point x'_n. Let $z_n = R_{\epsilon_n} x'_n$. Then we have $R_{-m_x} x_n = R_V R_{-m_z} z_n$. The centroid m_z is related to $m_{x'}$ and $\{\epsilon_n\}_{n \in [N]}$. Therefore, we can write $m_z = m_{x'} + \epsilon$ for a $\epsilon \in \mathbb{R}^d$. This leads to

$$R_{-m_x} x_n = R_V R_{\epsilon'_n} R_{-m_{x'}} x'_n, \ \forall n \in [N],$$

where $R_{\epsilon'_n} = R_{-m_{x'} - \epsilon} R_{\epsilon_n} R_{m_{x'}}$. If the translation noise of each point is sufficiently small, then $R_V R_{\epsilon'_n} \approx R_{V'}$ for a $V' \in \mathbb{O}(d)$.

B. Hyperbolic Rotation & Reflection

To estimate the unknown hyperbolic rotation, we consider minimizing a weighted discrepancy between the centered point sets. More precisely,

$$\widehat{U} = \underset{V \in \mathbb{O}(d)}{\arg\min} \sum_{n \in [N]} w_n f\left(d\left(R_{-m_x} x_n, R_V R_{-m_{x'}} x'_n\right)\right) \tag{4}$$

where $d(x, x') = \operatorname{acosh}(-x^\top H x')$, $\{w_n\}_{n \in [N]}$ are positive weights, and $f(\cdot) = \cosh(\cdot)$ is a monotonic function.

Proposition 2: The optimal unitary matrix that solves (4) equals $\widehat{U} = U_l U_r^\top$, where $U_l \Sigma U_r^\top$ is the singular value decomposition of $\mathcal{P}(R_{-m_x} X) W \mathcal{P}(R_{-m_{x'}} X')^\top$, and $W = \operatorname{diag}(w_1, \ldots, w_N)$.

Proof: We can simplify (4) as follows:

$$\widehat{U} = \underset{V \in \mathbb{O}(d)}{\arg\max} \sum_{n \in [N]} \operatorname{Tr} R_{-m_{x'}} x'_n w_n (R_{-m_x} x_n)^\top H R_V.$$

From Fact 1, we know that R_V is only parameterized on its lower right block. The proof then follows from representing the sum in matrix form and invoking von Neumann's trace inequality [31]. ∎

C. Möbius Addition

In the Poincaré model ($\mathbb{I}^d$), the points reside in the unit d-dimensional Euclidean ball. The isometry between the 'Loid and the Poincaré model $h : \mathbb{L}^d \rightarrow \mathbb{I}^d$ is called the *stereographic* *projection* [24]. The distance between $y, y' \in \mathbb{I}^d$ is given by $d(y, y') = 2\tanh^{-1}(\|-y \oplus y'\|)$ where $\oplus$ is Möbius addition — a noncommutative and nonassociative operator. *Gyration* measures the "deviation" of Möbius addition from commutativity, i.e., $\mathrm{gyr}[y, y'](y' \oplus y) = y \oplus y'$ [32].

Fact 2: The maps $h \circ R_U \circ h^{-1}$ and $h \circ T_U \circ h^{-1}$ are isometries in the Poincaré model, and they can be written as

$$h \circ T_U \circ h^{-1}(y) = Uy, \quad h \circ T_b \circ h^{-1}(y) = b' \oplus y$$

where $b' = h \circ \mathcal{Q}(b)$, T_b and T_U are defined in (2).

The translation isometry is a direct result of the Gyrotranslation theorem equality,

$$-(c \oplus y) \oplus c \oplus y' = \mathrm{gyr}[c, y](-y \oplus y'),$$

where $c \in \mathbb{I}^d$ [32]. Therefore, left Möbius addition preserves the distances of point sets in the Poincaré model. We can hence perform a Procrustes analysis in the Poincaré model by (1) centering each point set, i.e., subtracting their center of mass from the left hand side of the Möbius addition, and (2) estimating the remaining rotation factor — a composition of gyrations and the unknown rotation between the two point sets.

IV. Numerical Analysis

Let $x_n = R^* R_{\epsilon_n} x'_n, \ \forall n \in [N]$ where R^* is an H-unitary matrix and $\epsilon_1, \ldots, \epsilon_N$ is the set of translation noise samples. We consider the following three methods to compute an isometry that best matches the point sets X, X':

1) Hyperbolic Procrustes (P): The proposed method, for $W = 11^\top$, which returns the H-unitary matrix R_P.

2) Gradient descent (GD): Let us define the normalized discrepancy between X and $\overline{X}$ as $e(X, \overline{X}) \overset{\text{def}}{=} \frac{1}{Nd} \sum_{n \in [N]} d(x_n, \overline{x}_n)$. The matrix R_{GD} is computed by an iterative gradient descent method: We initialize $R_{\text{GD}} = I_{d+1}$, and iterate the following steps: (1) $\widehat{b} = -\alpha \frac{\partial}{\partial b} e(X, R_b R_{\text{GD}} X')|_{b=0}$ for a small $\alpha > 0$; (2) $\widehat{U} = \arg\max_{U \in \mathbb{O}(d)} \sum_{n \in [N]} [x_n, R_U R_{\widehat{b}} R_{\text{GD}} x'_n]$; (3) Update $R_{\text{GD}} \leftarrow R_{\widehat{U}} R_{\widehat{b}} R_{\text{GD}}$.

3) GD+P: The combination of previous methods by first solving the problem with our method, then fine-tuning the estimated isometry by the gradient method; This method returns $R_{\text{GD+P}}$.

For a random H-unitary R^* and all $n \in [N]$, we sample d-dimensional $z_n \sim \mathcal{N}(0, I)$ and $\epsilon_n \sim 10^{-2}\mathcal{N}(0, I)$; Then, we let $x'_n = \mathcal{Q}(z_n)$ and $x_n = R^* R_{\epsilon_n} x'_n$. For 10^3 randomly generated pairs (X, X'), we compute their normalized discrepancy $e(X, RX')$, where $R \in \{R_P, R_{\text{GD}}\}, R_{\text{GD+P}}$. All methods successfully denoise the measurements, i.e., $e(X, RX') < e(X, R^* X')$; see Fig. 4(a). However, the gradient descent method does not always converge to an acceptable solution. We define an outlier trial as follows

$$(X, X') : |e(X, RX') - Q_2| > k\frac{1}{2}|Q_3 - Q_1| \tag{5}$$

where Q_1, Q_2 and Q_3 are first, second and third quartiles of the total reported discrepancies, and $k = 5$ for a conservative criterion to pick outliers (see Fig. 4(b)). The gradient descent method has the most number of outliers (unstable solutions). On the opposite end, our proposed method has the minimum number of outliers — comparable to the number of outliers in the measurement noise. Therefore, the proposed close-form algorithm provides stable solutions for the hyperbolic Procrustes problem. And for noisy point sets — after removing the outlier trials — its accuracy is comparable to that of the gradient-based method and can be moderately improved with the post fine-tuning method.

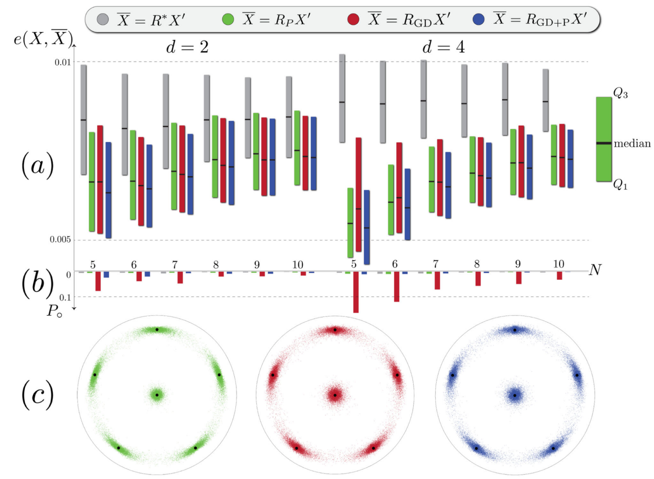

Fig. 4. (a) Normalized discrepancy for random hyperbolic point sets of size $N \in \{5, \ldots, 10\}$ and dimensions $d \in \{2, 4\}$. For 10^3 trials, we report the quartiles Q_1, Q_2 and Q_3 since they are robust to outliers. (b) The probability of an outlier event $P_\circ = 10^{-3} \times$ total number of outliers, e.g., the fraction of examples that failed to converge or outlier defined in the sense of (4). (c) Colored points shows the distribution of $\bar{X}$ compared to the true point set X (black), derived from R_P (green), R_{GD} (red), and $R_{\text{GD+P}}$ (blue) isometries.

Next, we devise an experiment to analyze the distribution of the erroneous matchings. For a fixed point set X, the six black points in Fig. 4(c), we generate 10^4 random noisy points X' which are related to X via random hyperbolic isometries and translation noises. In Fig. 4(c), we show the distribution of $\widehat{R}X'$ where $\widehat{R}$ is the H-unitary matrix computed by matching methods (1) to (3), as discussed earlier. Our proposed solution exhibits an larger angular and smaller radial variances in the matching errors $X - \widehat{R}X'$. However, this does not heavily impact the resulting discrepancy $e(X, \overline{X})$; see Fig. 4(a).

V. Conclusion

Inspired by its Euclidean counterpart, we introduced the Procrustes problem in hyperbolic spaces. Using the parameterized decomposition of hyperbolic isometries in terms of hyperbolic rotation and translation, we showed that how centering a point set makes them invariant to hyperbolic translation (for the case of no measurement noise). We then used the centered point sets to estimate the unknown rotation factor.

Acknowledgment

The authors would like to thank Prof. Olgica Milenković for helpful discussions and suggestions.

REFERENCES

[1] J. R. Hurley and R. B. Cattell, “The procrustes program: Producing direct rotation to test a hypothesized factor structure,” *Behav. Sci.*, vol. 7, no.2, pp. 258, 1962.

[2] J. C. Gower. “Generalized procrustes analysis,” *Psychometrika*, vol. 40, no.1, pp. 33–51, Mar. 1975.

[3] N. J. Mitra, N. Gelfand, H. Pottmann, and L. Guibas, “Registration of point cloud data from a geometric optimization perspective,” in *Proc. Eurograph./ACM SIGGRAPH Symp. Geometry Proc.*, pp. 22–31, 2004.

[4] J. M. Fitzpatrick, J. B. West, and Calvin R. Maurer, “Predicting error in rigid-body point-based registration,” *IEEE Trans. Med. Imag.*, vol. 17, no. 5, pp. 694–702, Oct. 1998.

[5] F. Pomerleau, F. Colas, and R. Siegwart, “A. review of point cloud registration algorithms for mobile robotics,” *Found. Trends Robot.*, vol. 4, no.1, pp. 1–104, 2015.

[6] I. Dokmanić, R. Parhizkar, J. Ranieri, and M. Vetterli, “Euclidean distance matrices: Essential theory, algorithms, and applications,” *IEEE Signal Process. Mag.*, vol. 32, no. 6, pp. 12–30, Nov. 2015.

[7] P. Tabaghi, I. Dokmanić, and M. Vetterli, “Kinetic Euclidean distance matrices,” *IEEE Trans. Signal Process.*, vol. 68, pp. 452–465, 2020.

[8] L. Liberti, C. Lavor, N. Maculan, and A. Mucherino, “Euclidean distance geometry and applications,” *SIAM Rev.*, vol. 56, no.1, pp. 3–69, 2014.

[9] P. Tabaghi and I. Dokmanić, “Hyperbolic distance matrices,” in *Proc. 26th ACM SIGKDD Int. Conf. Knowl. Discov. Data Mining, KDD 2020*, pp. 1728–1738.

[10] F. Sala, C. De Sa, A. Gu, and C. Ré, “Representation tradeoffs for hyperbolic embeddings,” in *Proc. Int. Conf. Mach. Learn.*, pp. 4460–4469, 2018.

[11] O.-E. Ganea, G. Bécigneul, and T. Hofmann, “Hyperbolic neural networks,” in *Proc. 32nd Int. Conf. Neural Informat. Process. Syst.*, 2018.

[12] O. Skopek, O.-E. Ganea, and G. Bécigneul, “Mixed-curvature variational autoencoders,” 2019, *arXiv:1911.08411*.

[13] P. Tabaghi, E. Chien, C. Pan, and O. Milenković, “Linear classifiers in mixed constant curvature spaces,” 2021, *arXiv:2102.10204*.

[14] W. Peng, T. Varanka, A. Mostafa, H. Shi, and G. Zhao, “Hyperbolic deep neural networks: A survey,” 2021, *arXiv:2101.04562*.

[15] M. Weber, M. Zaheer, A. S. Rawat, A. Menon, and S. Kumar, “Robust large-margin learning in hyperbolic space,” 2020, *arXiv:2004.05465*.

[16] B. Chen, X. Huang, L. Xiao, Z. Cai, and L. Jing, “Hyperbolic interaction model for hierarchical multi-label classification,” in *Proc. AAAI Conf. Arti. Intell.*, vol. 34, pp. 7496–7503, 2020.

[17] P. Shvaiko and J. Euzenat, “Ontology matching: State of the art and future challenges,” *IEEE Trans. Knowl. Data Eng.*, vol. 25, no.1, pp. 158–176, Jan. 2013.

[18] J. Euzenat, and P. Shvaiko, *Ontology Matching*, vol. 18. Berlin, Germany: Springer, 2007.

[19] Q. Lu *et al.*, “Learning electronic health records through hyperbolic embedding of medical ontologies,” in *Proc. 10th ACM Int. Conf. Bioinformat., Comput. Biol. Health Informat.*, 2019, pp. 338–346.

[20] D. Spohr, L. Hollink, and P. Cimiano, “A. machine learning approach to multilingual and cross-lingual ontology matching,” in *Proc. Int. Semant. Web Conf.*, pp. 665–680, Oct. 2011.

[21] H. Matsumoto, T. Mimori, and T. Fukunaga, “Novel metric for hyperbolic phylogenetic tree embeddings,” *Biol. Methods Protocols*, vol. 6, no. 1, 2021, Art. no. bpab006.

[22] D. Bogdanowicz and K. Giaro, “On a matching distance between rooted phylogenetic trees,” *Int. J. Appl. Math. Comput. Sci.*, vol. 23, no. 3, pp. 669–684, 2013.

[23] Y. Lin, V. Rajan, and B. M. E. Moret, “A metric for phylogenetic trees based on matching,” *IEEE/ACM Trans. Comput. Biol. Bioinf.*, vol. 9, no. 4, pp. 1014–1022, Jul./Aug. 2011.

[24] J. W. Cannon *et al.*, “Hyperbolic geometry,” *Flavors Geometry*, vol. 31, pp. 59–115, 1997.

[25] S. Rusinkiewicz and M. Levoy, “Efficient variants of the ICP algorithm,” in *Proc. Third Int. Conf. 3-D Digital Imag. Model.*, pp. 145–152, 2001.

[26] D. Alvarez-Melis, Y. Mroueh, and T. Jaakkola, “Unsupervised hierarchy matching with optimal transport over hyperbolic spaces,” in *Proc. Int. Conf. Artif. Intell. Statist.*, 2020, pp. 1606–1617.

[27] A. Hoyos-Idrobo, “Aligning hyperbolic representations: An optimal transport-based approach.” 2020, *arXiv:2012.01089*.

[28] K. V. Mardia and P. E. Jupp, *Directional Statistics*, vol. 494. Hoboken, NJ, USA: Wiley, 2009.

[29] I. Gohberg, P. Lancaster, and L. Rodman, “Matrices and indefinite scalar products,” *Operator Theory: Advances and Applications*, Basel, Switzerland: Birkhäuser, vol. 8, 1983.

[30] J. G. Ratcliffe, S. Axler, and K. A. Ribet, *Foundations of Hyperbolic Manifolds*, vol. 149. New York, NY, USA: Springer, 1994.

[31] L. Mirsky, “A trace inequality of John Von Neumann,” *Monatshefte für Mathematik* vol. 79, no. 4, pp. 303–306, 1975.

[32] A. Albert Ungar, “A gyrovector space approach to hyperbolic geometry,” *Synth. Lectures Math. Statist.*, vol. 1, no. 1, pp. 1–194, 2008.